JOURNAL OF SPACECRAFT AND ROCKETS
Vol. 42, No. 2, March–April 2005

Effective Modeling and Nonlinear Shell Analysis of Thin Membranes Exhibiting Structural Wrinkling

Alexander Tessler,* David W. Sleight,* and John T. Wang*
NASA Langley Research Center, Hampton, Virginia 23681-2199

Thin solar sail membranes of very large span are being envisioned for near-term space missions. One major design issue that is inherent to these very flexible structures is the formation of wrinkling patterns. Structural wrinkles may deteriorate a solar sail's performance and, in certain cases, structural integrity. A geometrically nonlinear, updated Lagrangian shell formulation is employed using the ABAQUS finite element code to simulate the formation of wrinkled deformations in thin-film membranes. The restrictive assumptions of true membranes as defined by tension field theory are not invoked. Two effective modeling strategies are introduced to facilitate convergent solutions of wrinkled equilibrium states. They include 1) the application of small, pseudorandom, out-of-plane geometric imperfections that ensure initiation of the requisite membrane-to-bending coupling in a geometrically nonlinear analysis and 2) the truncation of corner regions, where concentrated loads are prescribed, to improve load transfer, mesh quality, and kinematics and to reduce severe concentration of membrane stresses. The corner truncation necessitates replacing the concentrated force with a statically equivalent distributed traction. Several numerical studies are carried out, and the results are compared with recent experimental data. Good agreement is observed between the numerical simulations and experimental data.

Introduction

THE exploitation of solar energy for the purpose of near-term space exploration presents a viable and attractive possibility in the minds of NASA scientists and engineers. The specific propulsion technology is called solar sails. Very large, ultra-low-mass, thin-polymer film (gossamer) structures are now being designed and tested for a wide variety of space exploration missions. The difficulties associated with conducting tests in a weightless environment place greater emphasis on the reliance on computational methods. Other gossamer structures that possess similar structural characteristics include inflatable space antennas, sun shields, and radars. A concise overview of gossamer structures and related technologies can be found, for example, in Ref. 1.

A solar sail can gain momentum from incidence of sunlight photons at its surface. Because the momentum carried by an individual photon is very small, the solar sail must have a large surface area and a low mass, so that sufficient acceleration can be generated. Also, a solar sail requires a highly reflective surface that has minimal wrinkling and billowing under operational conditions. In the presence of significant wrinkling and billowing, the solar sail may lose efficiency, as compared to a flat sail, due to the oblique incidence of photons. The billowing problem may be overcome by applying sufficient tension to the sail membrane. Higher tensile stresses, however, are commonly accompanied by greater amplitude and longer structural wrinkles.

A thin-film solar sail is a classical two-dimensional structure, with a thickness that is much smaller than its lateral dimensions. Because the bending stiffness is negligibly small compared to its membrane stiffness, the load-carrying capability using thin, low-modulus films is predominantly due to tensile membrane stresses. One key response phenomenon intrinsic to this class of structures is structural wrinkling. Structural wrinkles are local postbuckling patterns that are manifested by geometrically large transverse deformations whose magnitudes are much larger than the membrane thickness. Their formation is generally attributed to extremely low compressive stresses supported by extremely low bending stiffness. To simulate such effects, the analytical model must necessarily account for both membrane and bending deformations undergoing geometrically nonlinear kinematics with large displacements and rotations, that is, a geometrically nonlinear shell model. However, obtaining stable equilibrium states using shell-based modeling turns out to be a challenging computational problem. Here, the elastic deformations, possessing a very small amount of strain energy, are accompanied by large rigid-body motions, rendering these structures underconstrained. Moreover, the shell models for these problems are highly ill-conditioned. The membrane rigidity, being much greater than the bending rigidity, may dominate excessively, thus, suppressing the formation of wrinkling deformations.

Because of the aforementioned analytical and computational challenges, most investigations of the analysis of thin membranes excluded the bending effect altogether, resulting in tension field (TF) theory applicable to the so-called true membranes.[2–16] By the elimination of compressive stresses through a modification of the constitutive relations, TF theory enables the prediction of the basic load transfer and wrinkle orientations in membranes; however, it cannot predict the out-of-plane wrinkled shapes, wavelengths, and amplitudes. Stein and Hedgepeth[6] explored a modified version of TF theory by identifying partially wrinkled domains. Following their methodology, Miller and Hedgepeth[10] performed a finite element analysis using a recursive stiffness-modification procedure termed the iterative membrane properties (IMP) method. In several computational efforts[11–16] the IMP and penalty-based formulations of TF theory were employed by implementing appropriate routines into the nonlinear finite element codes TENSION6[17,18] and ABAQUS.[19] The main utility of these TF approaches is to enable adequate load-carrying predictions to be made and to enable the general regions where structural wrinkles develop to be identified. The major shortcoming of the TF schemes, however, is their inability to predict the wavelengths and amplitudes of wrinkles. This shortcoming may be overcome by modeling thin-film structures using shell-based finite element analysis that includes both membrane and bending deformations.

Recent advances in nonlinear computational methods and shell-element technology offered viable possibilities of simulating highly nonlinear wrinkled deformations in thin membranes using shell-based analysis. Lee and Lee[20] developed a nine-node, quadratic

Presented as Paper 2003-1931 at the AIAA/ASME/ASCE/AHS 44th Structures, Structural Dynamics, and Materials Conference, Norfolk, VA, 7–10 April 2003; received 16 July 2003; accepted for publication 23 March 2004.

*Aerospace Engineer, Analytical and Computational Methods Branch, Structures and Materials Competency. Member AIAA.

shell element that used artificially modified shear and elastic moduli to enable locking-free shell analysis of very thin shells. They also employed small out-of-plane geometric imperfections using trigonometric functions. In addition, a fictitious damping term was added to the nonlinear equilibrium equations to circumvent numerical ill conditioning due to stability issues. They computed a wrinkled deformation state for a square membrane subjected two tensile forces; however, the numerical results were not validated with experiment. A similar computational effort using ABAQUS,[19] by Wong and Pellegrino,[21] involved the use of superposition of buckling eigenvectors to describe small out-of-plane geometric imperfections over the entire spatial domain of a membrane. They also provided some comparisons with experimental results. Neither of these efforts, however, examined how the application of various types of geometric imperfections and their spatial distributions may affect the outcome of a nonlinear analysis.

In this paper, several modeling ideas are explored for the purpose of aiding the geometrically nonlinear, updated Lagrangian shell analysis of thin-film membranes with emphasis on the wrinkled equilibrium/deformation state. The modeling ideas include 1) a simplified and computationally efficient way of introducing out-of-plane geometric imperfections, thus ensuring the necessary coupling between the membrane and bending deformations, and 2) identifying the tension-loaded corner regions as the critical modeling areas. Unless adequate meshing and load introduction are used, these regions can effectively lock the wrinkling formation due to an overly stiff behavior. The undesirable stiffening may also be directly linked to the boundary restraints in the corner regions, thus, preventing the formation of wrinkles.

Several numerical studies are carried out using the ABAQUS code. These studies include analyses of 1) a flat rectangular membrane loaded in shear and 2) a flat square membrane loaded in tension by corner forces. Relevant parametric studies of geometric imperfections are performed and provide an improved insight on their use in the geometrically nonlinear analysis of thin membranes. Comparisons with experimental results are also provided and discussed.

Analysis Framework and Modeling Strategies

Elastic, quasi-static shell analyses and parametric studies of thin-film membranes loaded in plane are carried out using the geometrically nonlinear (GNL), updated Lagrangian description of equilibrium formulation implemented in ABAQUS.[19]

The selection of a four-node, shear-deformable shell element, S4R5, incorporating large-displacement and small-strain assumptions, is made because of the following considerations. The element is based on Mindlin theory and uses C^0-continuous bilinear interpolations of the kinematic variables. To allow adequate modeling of thin-shell bending, the element employs reduced integration of the transverse shear energy and an ad hoc correction factor that multiplies the transverse shear stiffness. The latter device imposes the Kirchhoff constraints, that is, zero transverse shear strains, numerically. Both of these computational remedies are intended to facilitate locking-free bending deformations in thin shells. To improve the element's reliability, an hourglass control method is used to suppress spurious zero-energy (hourglass) modes that result from underintegrating the shear strain energy. Such low-order, C^0-continuous shell elements are commonly preferred for nonlinear analysis because of their computational efficiency, robustness, and superior convergence characteristics.

For a localized structural instability such as wrinkling, the ABAQUS code provides a volume-proportional numerical damping scheme invoked by the STABILIZE parameter. The stabilization feature adds fictitious viscous forces to the global equilibrium equations. This enables the computation of finite displacement increments in the vicinity of unstable equilibrium and, thus, circumvents numerical ill-conditioning due to stability issues. The default value of the stabilization parameter (2.0×10^{-4}) is used in the numerical examples that follow.

Next, quasi-static shell solutions for two thin-film membranes are discussed. The deformations in these membranes are associated with the highly nonlinear, low-strain-energy equilibrium states that possess structural wrinkles. Enabling modeling strategies for the solution of these computationally challenging problems are discussed.

Application of Pseudorandom Geometric Imperfections

When planar membranes are subjected to purely in-plane loading, no mechanism exists, even in the presence of compressive stresses, to initiate the out-of-plane, buckled deformations. One way to overcome this difficulty is to perturb slightly the planar geometry out of plane. In this manner, the geometric perturbations (imperfections) will engender the necessary coupling between the bending and membrane deformations.

In this effort, to initiate the requisite membrane-to-bending coupling, pseudorandom geometric imperfections are imposed at the nodes of the originally planar membrane mesh. The computing effort involved in generating such a set of pseudorandom numbers is trivial. In the simplest setting, the imperfections can be applied at every interior node of the mesh, and the imperfection magnitudes may be computed as a function of the membrane thickness as

$$z_i = \alpha \delta_i h \qquad (i = 1, N) \tag{1}$$

where α is a dimensionless amplitude parameter, $\delta_i \epsilon [-1, 1]$ is a pseudorandom number, h is the membrane thickness, and N is the number of nodes with the imposed imperfections. As will be subsequently demonstrated, there are many alternative ways of spatially distributing these imperfections and choosing the value of α.

The imperfection amplitudes z_i that are regulated by α need to be sufficiently small in relation to the element size to avoid excessive out-of-plane element distortions; this is particularly significant for planar elements with four or more nodes. To preserve a nearly flat membrane, z_i may need to be small in comparison to the membrane thickness. However, z_i should be large enough to enable adequate coupling to take place between membrane and bending deformations. This aspect is quantified in a parametric study that follows.

The randomness aspect of Eq. (1) ensures an unbiased imperfection pattern. Thus, the imperfections neither predefine nor dominate the resulting deformed equilibrium state. Geometric imperfections are commonly specified over the whole spatial domain of a membrane, for example, as in Refs. 20 and 21. As demonstrated subsequently, strategic application of geometric imperfections over partial mesh regions may also be just as effective. This further points out that conducting a computationally intensive analysis to generate geometric imperfections based on a related structural problem, such as a buckling eigenvalue problem in Ref. 21, may be entirely unnecessary.

Square Thin-Film Membrane Subjected to In-Plane Shear Loading

The choice of the first numerical example is primarily motivated by the availability of recent experimental data obtained by Leifer and his colleagues at NASA Langley Research Center using the photogrammetry technique. (Refer to Leifer et al.[22]) The problem is closely analogous to that reported in Ref. 21. The geometry and

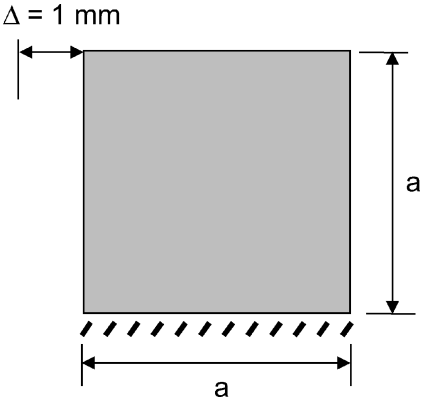

Fig. 1 Square thin-film membrane (Mylar film) clamped along bottom edge and subjected to prescribed displacement along top edge.

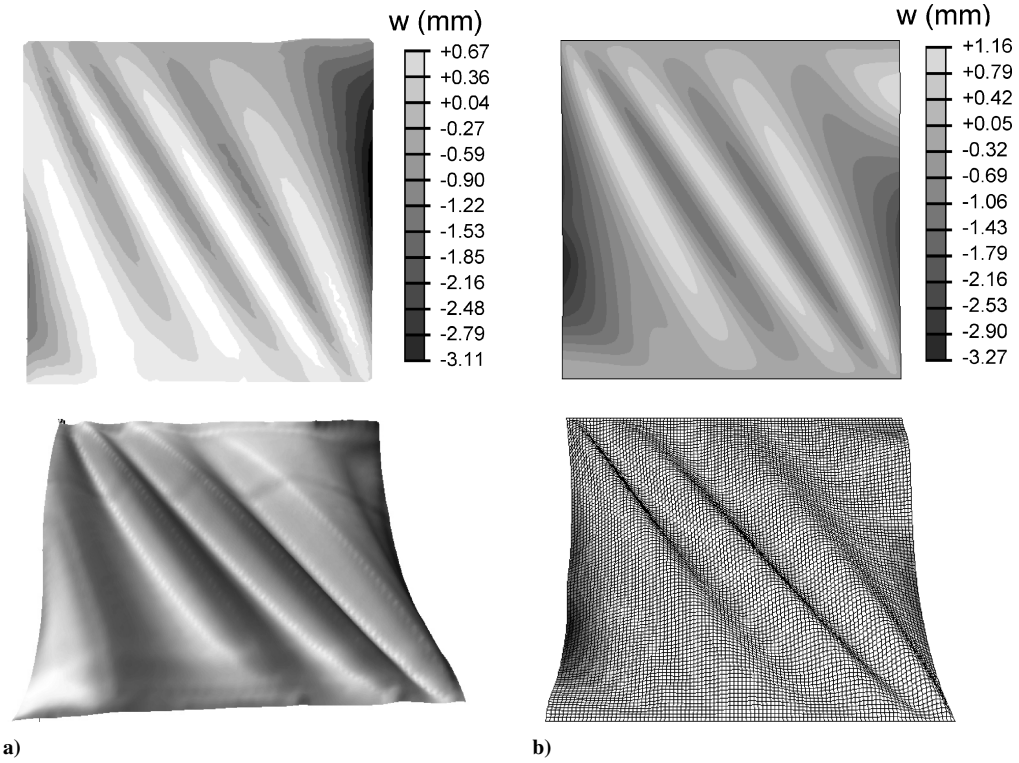

Fig. 2 Wrinkling deformations of clamped, square, thin-film membrane (Mylar film) subjected to prescribed displacement along top edge: a) experiment (photogrammetry)[22] and b) GNL/finite element method shell analysis (ABAQUS, S4R5).

loading are shown in Fig. 1, where a square membrane (Mylar® polyester film, edge length $a = 229$ mm, thickness $h = 0.0762$ mm, elastic modulus $E = 3790\,\mathrm{N/mm^2}$, and Poisson's ratio $\nu = 0.38$) is clamped along the bottom edge and subjected to a uniform horizontal displacement of 1 mm along the top edge. The span-to-thickness ratio (a/h) of the membrane is approximately 3×10^3 and, from the perspective of shell theory, the membrane is regarded as a thin shell. Based on results of a preliminary convergence study (not discussed herein), a highly refined mesh is constructed of 10^4 square-shaped S4R5 shell elements. The numerical model that is originally planar is augmented by the pseudorandom, nodal imperfections distributed over the interior nodes of the model, using the amplitude parameter $\alpha = 0.1$. A sample of the ABAQUS input data for this analysis is provided in Appendix A. In Fig. 2, the out-of-plane deformation contours are shown and demonstrate a relatively close agreement between the experiment and analysis in terms of the number of wrinkles, their orientation, and their amplitudes. The amplitude of the left-edge wrinkle deflecting downward, which represents the maximum wrinkle amplitude, compares within 5% between the experiment and analysis. Note, however, that in the experiment, the Mylar film was slightly curved out-of-plane before the application of the horizontal displacement. This actual initial imperfection was not included in the computational model given that the main focus of this analysis was to validate the efficacy of the pseudorandom imperfection approach. Naturally, provided that the actual initial imperfections are adequately measured before loading, they should be included in a computational model.

Square Thin-Film Membrane Subjected to Symmetric Corner Tensile Loads

When a tensile load is applied at a corner of a thin-film membrane, wrinkles tend to radiate from the corner; subsequently, the corner wrinkling affects the wrinkled equilibrium state over the entire membrane domain.

Recently, Blandino et al.[23] performed a laboratory test on a 500-mm square, flat membrane made of a Kapton® type HN film. The membrane dimensions and loading are shown in Fig. 3. The membrane properties are edge length $a = 500$ mm, thickness

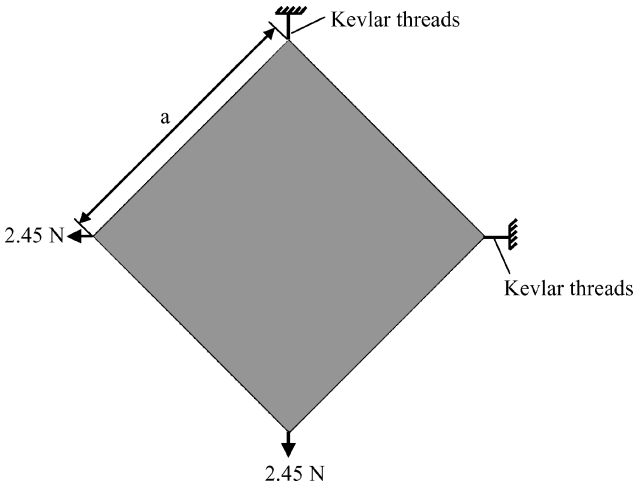

Fig. 3 Square thin-film membrane (Kapton type HN film) loaded in tension by corner forces as tested by Blandino et al.[23]

$h = 0.0254$ mm, elastic modulus $E = 2590\,\mathrm{N/mm^2}$ and Poisson's ratio $\nu = 0.34$. The membrane is subjected to tensile corner loads ($F = 2.45$ N) applied in the diagonal directions via Kevlar® threads at the left and bottom corners of the membrane. The top and right corners of the membrane are fixed to the test frame with Kevlar threads. The corners are also reinforced on both sides with small patches of a transparency film (approximately 10 mm in diameter).

A suitable analytical model that is statically equivalent to the experimental one would result in the loading by four tension corner forces acting in the opposite directions along the two diagonals of the square membrane. In a computational shell model, specifying the applied concentrated forces at the corner nodes does not lead to a wrinkled equilibrium state, even with the inclusion of the geometric imperfections discussed in the preceding example. Here, two model-related pitfalls that prevent the development of wrinkling can be inferred. First, a concentrated corner force, causing a near-singular

membrane stress field, may bring about pathological performance in the neighboring elements because conventional elements cannot model singular stress fields. Thus, the dominant membrane strain energy may suppress an already very small bending energy, causing severe ill conditioning and eliminating the influence of the local bending energy altogether. The second modeling concern is of kinematical nature. The corner elements are often distorted, meeting at a single corner node, that is, quadrilaterals collapsed into triangles, at which kinematic boundary conditions may be imposed. Tessler[24] demonstrated, in closed form and numerically, that acute bending stiffening (and even shear locking) may result in otherwise perfectly well-performing Mindlin elements strictly due to overconstraining of the element kinematics because of the nodal restraints. This severe bending stiffening results from the Kirchhoff constraints (zero transverse shear strain conditions) that engender spurious kinematic relations in the elements situated along the boundaries (and lines of symmetry) where the kinematic restraints are imposed. Consequently, with the overconstrained, stiff corners, no wrinkling can be initiated.

The preceding arguments lead to a basic conclusion that eliminating sharp-corner meshes, in the regions where concentrated loads are applied, may be beneficial for the modeling of wrinkled equilibrium states. Truncating a corner a short distance inward may result in an improved load transfer and mesh quality in that local region. This truncation will necessitate replacing the concentrated force with a statically equivalent distributed traction. The benefits of this strategy are twofold: First is the removal of a severe stress concentration. (Note that, in practice, the load introduction into a structure is closer to a distributed load than a concentrated force.) The second benefit is the improvements in the kinematics in the critical corner regions from which wrinkles radiate.

Consistent with the present modeling philosophy, the corners of the square membrane are cutoff such that the length of each corner edge (which is normal to the direction of the applied load) is set to be small, as shown in Fig. 4. The prescribed kinematic boundary restraints are also depicted in the figure. The domain of the entire membrane is discretized with a relatively refined mesh (4720 elements) for suitable comparison with the experiment. For simplicity and for validating the efficacy of the corner cutoff modeling, the reinforced corners of the membrane are not modeled. Also excluded from the model are the actual out-of-plane imperfections of the membrane surface, the asymmetries associated with the load introduction, and the effect of gravity. Therefore, with such simplifying modeling assumptions, it is only reasonable to expect a relatively good qualitative correlation with the experiment. On the other hand, by modeling the corner reinforcements used in the experiment and by accounting for the actual geometric imperfections and gravity incurred in the experimental setup, a reasonably good quantitative correlation with the experiment should be expected. The originally planar finite element mesh is augmented by the pseudorandom, nodal imperfections distributed over the interior nodes of the model, using the amplitude parameter $\alpha = 0.1$ (A parametric study on the selection of α is discussed subsequently.) A sample of the ABAQUS input data for this analysis is given in Appendix B.

The deflection distributions in the experiment and the present geometrically nonlinear shell analysis are shown in Fig. 5. The computer simulation is able to predict effectively four wrinkles radiating from the truncated corner regions just as those from the measured experimental results. The analysis also shows that curling occurs at the free edges as observed in the experimental results; however, the amplitudes of the experimental deflections are somewhat greater. Although intended to be symmetric, the experimental results are somewhat asymmetric. As in the earlier example, the actual initial geometric imperfections, not incorporated in the analysis, may have contributed to a significant asymmetry in the experiment and the differences with the analysis. This again shows that such ultraflexible and lightly stressed spatial structures are not only difficult to model analytically but also to test experimentally, requiring further refinements in the experimental methods for these thin-film membranes.

Study of Imperfection Amplitudes

The practical question of how to decide on the appropriate value of the amplitude parameter α in Eq. (1) may be satisfactorily answered through a parametric study in which the distribution of the pseudorandom imperfections is kept constant and the value of α is varied. To minimize the computational effort, it suffices to model a symmetric quadrant of the membrane as shown in Fig. 6, where the imperfections are defined over all interior nodes. The appropriate truncations of the corners, the application of statically equivalent distributed tractions, and the symmetry boundary conditions are all implemented as already described.

The amplitude parameter α is varied in the range $0.001 \leq \alpha \leq 5.0$, and for each fixed value of this parameter, a geometrically nonlinear analysis is performed. The results from this study are presented

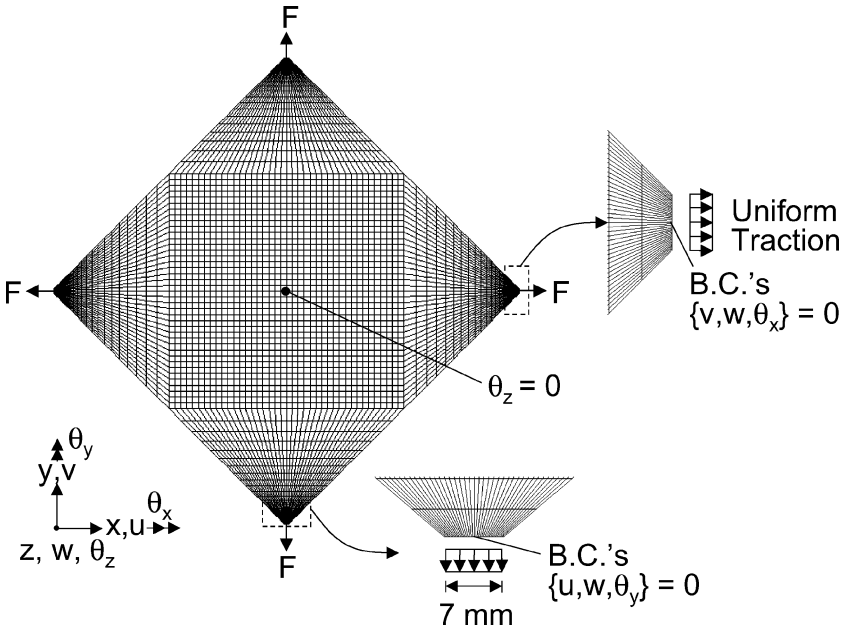

Fig. 4 Square thin-film membrane (Kapton type HN film) loaded in tension by corner tractions: full finite element method model with truncated corners using GNL S4R5 shell elements in ABAQUS code.

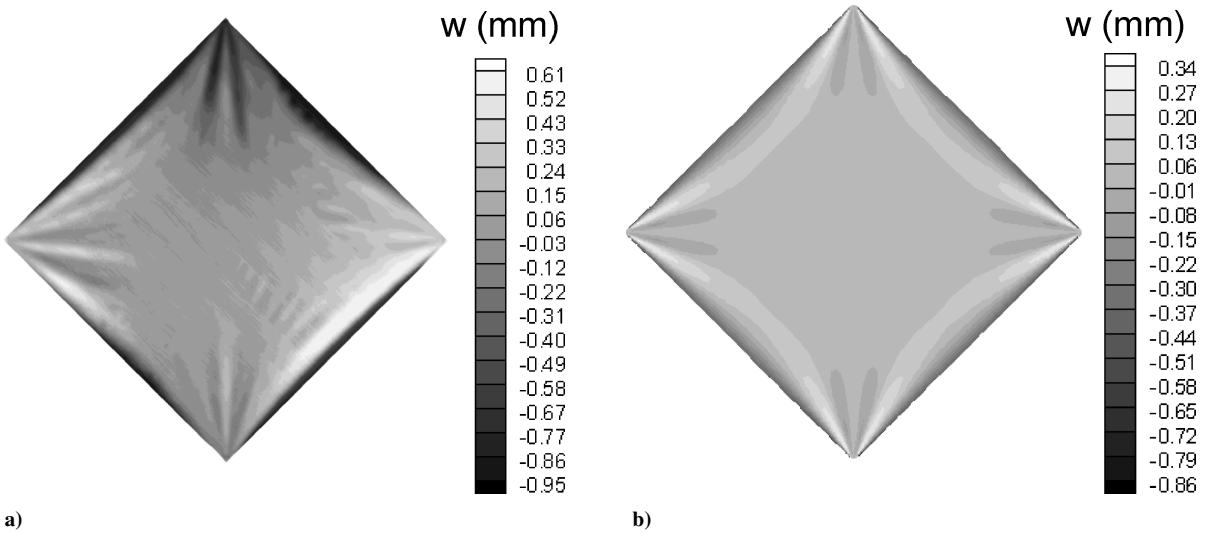

Fig. 5 Wrinkling deformations of square thin-film membrane (Kapton type HN film) loaded in tension by corner tractions: a) experiment (capacitance sensor measurement)[23] and b) GNL/finite element method shell analysis (ABAQUS, S4R5).

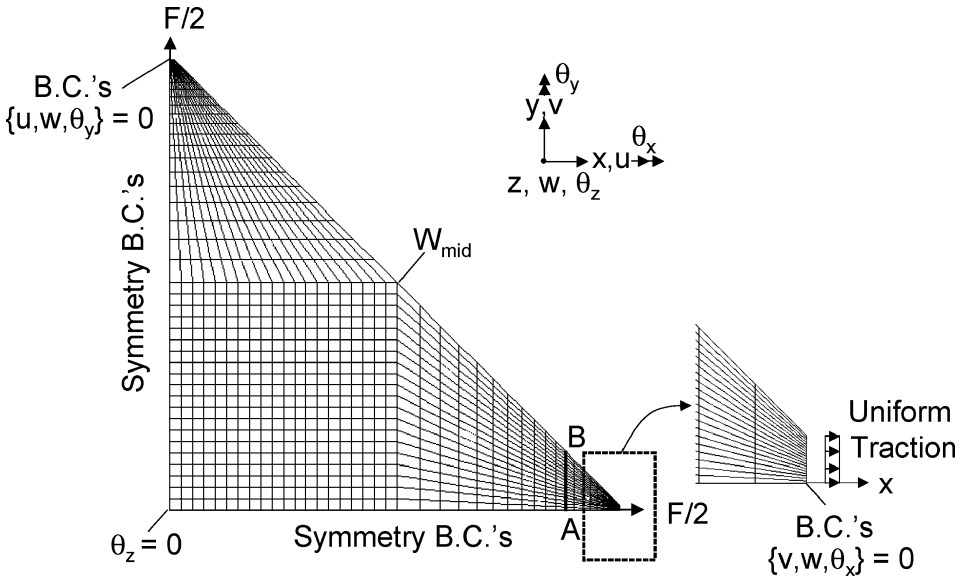

Fig. 6 Square thin-film membrane (Kapton type HN film) loaded in tension by corner tractions: symmetric-quadrant model with truncated corners used in parametric studies.

in Fig. 7, where a normalized deflection, W_{mid}/h, at the center of the membrane free edge (and which represents the maximum value of the deflection across the entire domain) is plotted vs α. There are three basic ranges in the graph. For very small amplitudes ($\alpha < 0.005$), the imperfections are not large enough to provide sufficient bending-to-membrane coupling. No wrinkling deformations can be simulated. In the range $0.01 \leq \alpha \leq 1.0$, all analyses predict practically the same wrinkled deformation equilibrium state as evidenced by the constant value of W_{mid}/h across this range of α. The solutions corresponding to the values $\alpha > 1$ can be viewed as erroneous because this range of α values implies that the imperfection amplitudes are too large; in fact, they are on the order of the membrane thickness. One way to interpret this is by examining the transverse element distortions that may have been caused by the large imperfections: In general, one of the four element nodes will be out-of-plane, thus, violating the basic element formulation.

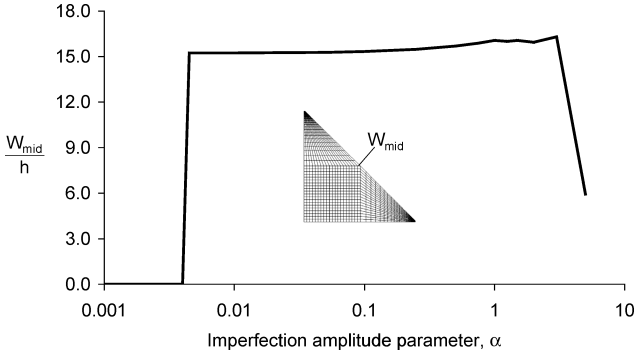

Fig. 7 Square thin-film membrane (Kapton type HN film) loaded in tension by corner tractions: effect of imperfection amplitude on the development of wrinkling deformations in GNL/finite element method shell models.

Study of Spatial Distribution of Imperfections

In this study, several alternative schemes of spatial distributions of the imperfections are examined in relation to their effect on the

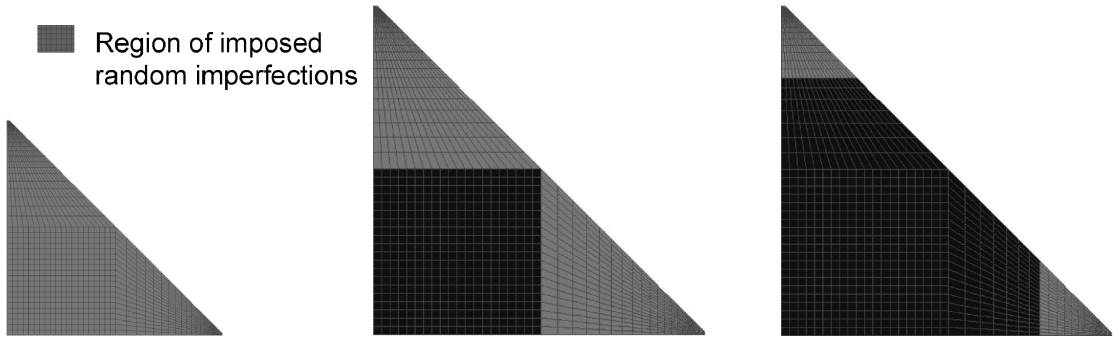

a) Imperfection model 1 b) Imperfection model 2 c) Imperfection model 3

Fig. 8 Square thin-film membrane (Kapton type HN film) loaded in tension by corner tractions: symmetric-quadrant GNL/finite element method shell models showing regions of imposed random imperfections.

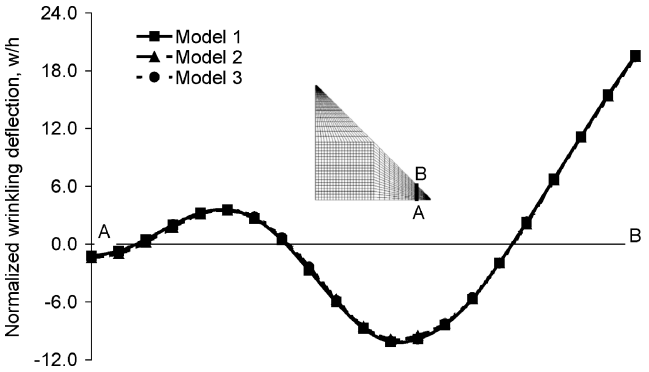

Fig. 9 Square thin-film membrane (Kapton type HN film) loaded in tension by corner tractions: wrinkling deflection along section A–B corresponding to three imperfection models for a fixed value of the imperfection amplitude parameter $\alpha = 0.10$.

wrinkled equilibrium states. Consider three distinct imperfection distribution models corresponding to $\alpha = 0.10$ (from the acceptable range of values), as shown in Fig. 8. In model 1, the imperfections are imposed across all of the interior nodes (in the shaded region). In models 2 and 3, the imperfections are only focused on the corner regions. The results from this study are presented in Fig. 9, which shows a wrinkled wave along the A–B line (Fig. 6). Noticeably, the three imperfection schemes produce the same wrinkled deformations, and this is consistent across the whole membrane. Thus, the imperfection schemes may be deemed equivalent from the perspective of determining the appropriate wrinkled deformations for this problem. This is not surprising because the dominant wrinkling modes emanate from the corner regions. For this reason, the imperfections need only be imposed over these key regions.

Conclusions

Careful modeling considerations were explored to simulate the formation of highly nonlinear wrinkling deformations in thin-film membranes. The analyses were carried out within the framework of the geometrically nonlinear, updated Lagrangian shell formulation using a commercial finite element code ABAQUS. The underlying shell relations employ the assumptions of small strains and large displacements and do not rely on the classical membrane assumptions of TF theory. The finite element models utilize a Mindlin-type quadrilateral shell element, S4R5. The element employs reduced integration of the transverse shear energy and has an ad hoc correction factor multiplying the shear stiffness to ensure locking-free bending behavior even for very thin shells. Moreover, the hourglass control scheme is used to suppress spurious zero-energy (hourglass) modes that result as a consequence of the reduced integration.

To achieve convergent geometrically nonlinear solutions that correlate well with experiment, the issue of deformation coupling between bending and membrane deformation was addressed. By the application of pseudorandom out-of-plane imperfections to the initially planar membrane surface, the requisite membrane-to-bending coupling is invoked at the commencing stage of the nonlinear solution process. When relatively small and unbiased imperfections are used, converged wrinkled equilibrium states can be obtained that are independent of the initial imperfections.

For the class of thin-film problems in which corner regions are subjected to tension loads, as in the second example problem, the need for improved modeling of such corner regions was identified. The introduction of truncated corners and the replacement of concentrated loads with statically equivalent distributed tractions enabled successful geometrically nonlinear wrinkled stress states to be determined.

The present modeling schemes were used in several numerical studies involving thin-film membranes subjected to mechanical loads. First, converged wrinkled deformation modes were predicted for a square membrane loaded in shear. These results compared favorably with an experiment recently conducted at NASA Langley Research Center. In the second example, a square membrane subjected to four-corner tensile loads was analyzed and exhibited major wrinkling emanating from the corners. The corner regions were truncated in the model to design out the near singular stress fields associated with concentrated loads and to improve element topology to avoid overly stiff corners. A noticeably close correlation with the experiment was also observed for this very challenging computational problem. It is expected that even closer correlation may be possible once the actual corner reinforcements and geometric imperfections, including the effect of asymmetry of the load introduction, are represented in a computational model in sufficient detail. Also, a greater insight was developed through a set of parametric studies of the amplitudes and spatial distributions of the pseudorandom imperfections.

Our experience with the geometrically nonlinear, updated Lagrangian shell analysis of thin-film membranes suggests that the current state-of-the-art computational methods have the potential for adequately simulating the structural response of such highly flexible and underconstrained wrinkled structures. There exist, however, numerous challenging issues requiring in-depth analytic, computational, and experimental pursuits. Issues related to robustness, nonlinear solution convergence, sensitivity to boundary restraints and applied loading, mesh dependence, and the shell-element technology, specifically addressing ultrathin behavior, need to be closely examined and addressed. Computational opportunities also exist in exploring the explicit dynamics nonlinear analyses that may have the advantage of obviating the stability issues in modeling the wrinkling phenomenon.

Appendix A: Input Files for Square Thin-Film Membrane Subjected to In-Plane Shear Loading

Main Input File

```
*HEADING
**
** Main input file named ‘‘Square Thin-Film Membrane Subjected to In-plane
** Shear Loading". Use is made of pseudorandom imperfections in the range of
**(-1/+1)times the thickness.
**
*RESTART, WRITE, FREQUENCY=1
**
*NODE
       1,        -114.3,        -114.3
       2,      -112.014,        -114.3
       3,      -109.728,        -114.3
       4,      -107.442,        -114.3
       5,      -105.156,        -114.3
       6,       -102.87,        -114.3
**
** To shorten the input listing, numerous NODE data
** lines are not shown. There are 10201 nodes in this model.
**
   10196,        102.87,         114.3
   10197,       105.156,         114.3
   10198,       107.442,         114.3
   10199,       109.728,         114.3
   10200,       112.014,         114.3
   10201,         114.3,         114.3
**
*ELEMENT, TYPE=S4R5, ELSET=MEMBRANE
       1,       1,       2,     103,     102
       2,       2,       3,     104,     103
       3,       3,       4,     105,     104
       4,       4,       5,     106,     105
       5,       5,       6,     107,     106
**
** To shorten the input listing, numerous ELEMENT data
** lines are not shown. There are 10,000 elements in this model.
**
    9995,   10094,   10095,   10196,   10195
    9996,   10095,   10096,   10197,   10196
    9997,   10096,   10097,   10198,   10197
    9998,   10097,   10098,   10199,   10198
    9999,   10098,   10099,   10200,   10199
   10000,   10099,   10100,   10201,   10200
**
** Membrane
**
*SHELL SECTION, ELSET=MEMBRANE, MATERIAL=MYLAR
      0.0762,       5
**
*MATERIAL, NAME=MYLAR
**
*ELASTIC, TYPE=ISO
       3790.,        0.38
*DENSITY
1.39E-6,
**
** Clamped
**
*BOUNDARY, OP=NEW
CLAMPED, ENCASTRE
**
*IMPERFECTION,SYSTEM=R,INPUT= Shear-imperfections.inp
**
** Step 1, Nonlinear
** Load Case, Default
**
*STEP, AMPLITUDE=RAMP, INC=250, NLGEOM
Nonlinear 1
*STATIC,STABILIZE
        0.01,          1.,       1.E-6,         0.1
```

```
**
*CONTROLS,PARAMETERS=TIME INCREMENTATION
50,50,15,50,,,,20
**
*NSET, NSET=CLAMPED, GENERATE
       1,     101,       1
*NSET, NSET=SHEAR, GENERATE
   10101,   10201,       1
**
** 1mm_Shear
**
*BOUNDARY
SHEAR, 1,,         -0.50
SHEAR, 2,6,          0.
**
*NODE PRINT, FREQ=1
U,
*NODE FILE, FREQ=1
U,
**
*EL PRINT, POS=INTEG, FREQ=1
S,
E,
**
*EL PRINT, POS=INTEG, FREQ=1, ELSET=MEMBRANE
         2,         3,         4,
S,
E,
*EL FILE, DIR=YES, POS=INTEG, FREQ=1
S,
E,
**
*EL FILE, DIR=YES, POS=INTEG, FREQ=1, ELSET=MEMBRANE
         2,         3,         4,
S,
E,
**
*EL FILE, DIR=YES, POS=NODES, FREQ=0
*EL FILE, DIR=YES, POS=CENTR, FREQ=0
*EL FILE, POS=AVERAGE, FREQ=0
*MODAL FILE, FREQ=99999
*ENERGY FILE, FREQ=0
*PRINT, FREQ=1
*END STEP
**
** Step 2, Nonlinear
** Load Case, Default
**
*STEP, AMPLITUDE=RAMP, INC=250, NLGEOM
Nonlinear 2
*STATIC,STABILIZE
        0.01,          1.,       1.E-6,         0.1
**
*NSET, NSET=CLAMPED, GENERATE
       1,     101,       1
*NSET, NSET=SHEAR, GENERATE
   10101,   10201,       1
**
** 1mm_Shear
**
*BOUNDARY
SHEAR, 1,,         -1.0
**
*NODE PRINT, FREQ=1
U,
*NODE FILE, FREQ=1
U,
**
*EL PRINT, POS=INTEG, FREQ=1
S,
E,
```

```
**
*EL PRINT, POS=INTEG, FREQ=1, ELSET=MEMBRANE
         2,         3,         4,
S,
E,
*EL FILE, DIR=YES, POS=INTEG, FREQ=1
S,
E,
**
*EL FILE, DIR=YES, POS=INTEG, FREQ=1, ELSET=MEMBRANE
         2,         3,         4,
S,
E,
**
*EL FILE, DIR=YES, POS=NODES, FREQ=0
*EL FILE, DIR=YES, POS=CENTR, FREQ=0
*EL FILE,  POS=AVERAGE, FREQ=0
*MODAL FILE, FREQ=99999
*ENERGY FILE, FREQ=0
*PRINT, FREQ=1
**
*END STEP
```

Geometric Imperfection Input File

```
**
** This file named ‘‘Shear-imperfections.inp" contains pseudorandom
** imperfections specified at the nodes in the z-direction. This file is
** called from the main input file named ‘‘Shear-membrane.inp".
**
** X, Y, and Z imperfections to be added to the nodal coordinates
  103,   0.00000E+00,   0.00000E+00,  -0.15770E-02
  104,   0.00000E+00,   0.00000E+00,   0.23648E-02
  105,   0.00000E+00,   0.00000E+00,  -0.87082E-03
  106,   0.00000E+00,   0.00000E+00,  -0.48120E-03
  107,   0.00000E+00,   0.00000E+00,  -0.61240E-03
  108,   0.00000E+00,   0.00000E+00,  -0.20922E-02
  109,   0.00000E+00,   0.00000E+00,   0.15041E-02
**
** To shorten the input listing, numerous NODE data
** lines are not shown. There are 10201 nodes in this model.
**
10093,   0.00000E+00,   0.00000E+00,   0.24146E-02
10094,   0.00000E+00,   0.00000E+00,  -0.22184E-02
10095,   0.00000E+00,   0.00000E+00,  -0.17705E-02
10096,   0.00000E+00,   0.00000E+00,   0.16460E-02
10097,   0.00000E+00,   0.00000E+00,  -0.24509E-03
10098,   0.00000E+00,   0.00000E+00,   0.17786E-02
10099,   0.00000E+00,   0.00000E+00,  -0.67721E-03
```

Appendix B: Input Files for Square Thin-Film Membrane Subjected to Symmetric Corner Tensile Loads

Main Input File

```
*HEADING
**
** Main input file named ‘‘Tension-membrane.inp" for ‘‘Square Thin-Film
** Membrane Subjected to Symmetric Corner Tensile Loads". Use is made of
** pseudorandom imperfections in the range of (-1/+1) times thickness
**
*NODE
       1,       3.51797,       350.035
       2,       7.34692,       346.206
       3,       11.5143,       342.039
       4,       16.0501,       337.503
       5,       20.9869,       332.566
       6,       26.3601,       327.193

**
**     To shorten the input listing, numerous NODE data
**     lines are not shown. There are 1323 nodes in this model.
**
    1318,       350.035,       2.63847
    1319,       350.035,       2.81437
```

```
    1320,       350.035,       2.99027
    1321,       350.035,       3.16617
    1322,       350.035,       3.34207
    1323,       350.035,       3.51796
**
**
*ELEMENT, TYPE=S4R5, ELSET=MEMBRANE
       1,       1,      21,      22,       2
       2,       2,      22,      23,       3
       3,       3,      23,      24,       4
       4,       4,      24,      25,       5
       5,       5,      25,      26,       6
       6,       6,      26,      27,       7
**
**     To shorten the input listing, numerous ELEMENT data
**     lines are not shown. There are 1200 elements in this model.
**
    1193,    1294,    1315,    1316,    1295
    1194,    1295,    1316,    1317,    1296
    1195,    1296,    1317,    1318,    1297
    1196,    1297,    1318,    1319,    1298
    1197,    1298,    1319,    1320,    1299
    1198,    1299,    1320,    1321,    1300
    1199,    1300,    1321,    1322,    1301
    1200,    1301,    1322,    1323,    1302
**
** membrane
**
*SHELL SECTION, ELSET=MEMBRANE, MATERIAL=MAT-TEST
      0.0254,       5
**
** mat-test
**
*MATERIAL, NAME=MAT-TEST
**
*DENSITY
      1.42E-6,
**
*ELASTIC, TYPE=ISO
**       2.6E+3,         0.3
       2590.0,         0.34
**
*NSET, NSET=DISP-TOP,GENERATE
1,401,20
*NSET, NSET=DISP-RT,GENERATE
1303,1323,1
*NSET, NSET=DISP-MID
20
*NSET, NSET=DISP-OUT,GENERATE
1051,1071,1
*NSET, NSET=DISP-END
     401,1303
*NSET, NSET=DISP-CEN
     861,
*NSET, NSET=DISP-BOT
     441,     462,     483,     504,     525,     546,     567,     588,
     609,     630,     651,     672,     693,     714,     735,     756,
     777,     798,     819,     840,     925,     946,     967,     988,
    1009,    1030,    1051,    1072,    1093,    1114,    1135,    1156,
    1177,    1198,    1219,    1240,    1261,    1282,     1303
*NSET, NSET=DISP-LEF, GENERATE
     401,     420,       1
     842,     860,       1
*NSET, NSET=FORCE-X, GENERATE
    1304,    1322,       1
*NSET, NSET=HALF-FX
    1303,    1323
*NSET, NSET=FORCE-Y
      21,      41,      61,      81,     101,     121,     141,
     161,     181,     201,     221,     241,     261,     281,     301,
     321,     341,     361,     381
```

```
*NSET, NSET=HALF-FY
      1,      401
**
** disp-center
**
*BOUNDARY
DISP-CEN, 1,,          0.
DISP-CEN, 2,,          0.
**
*BOUNDARY
DISP-CEN, 4,,          0.
DISP-CEN, 5,,          0.
DISP-CEN, 6,,          0.
**
** disp-bot
**
*BOUNDARY
DISP-BOT, YSYMM
**
** disp-left
**
*BOUNDARY
DISP-LEF, XSYMM
**
** disp-end
**
*BOUNDARY
DISP-END, 3,,          0.
**
** Step 1, nonlinear
** Load Case, Default
**
*IMPERFECTION, SYSTEM=R,INPUT=Tension-imperfections.inp
*STEP, AMPLITUDE=RAMP,INC=5000,NLGEOM
Nonlinear Static Analysis
**
This load case is the default load case that always appears
**
*STATIC
0.01,1.0,1.0E-6,0.10
**
** force-x
**
*CLOAD
FORCE-X, 1,          6.125E-2
**
** half-force-x
**
*CLOAD
HALF-FX, 1,          3.0625E-2
**
** force-y
**
*CLOAD
FORCE-Y, 2,          6.125E-2
**
** half-force-y
**
*CLOAD
HALF-FY, 2,          3.0625E-2
**
**
*NODE PRINT, TOTALS=YES,FREQ=1
U,
RF
**
*NODE PRINT, TOTAL=YES,FREQ=1, NSET=DISP-TOP
U,
*NODE PRINT, TOTAL=YES,FREQ=1, NSET=DISP-RT
U,
*NODE PRINT, FREQ=1, NSET=DISP-MID
```

```
U,
*EL PRINT, POS=CEN, FREQ=1
S,
E,
**
*END STEP
```

Geometric Imperfection Input File

```
**
** This file named ‘‘Tension-imperfections.inp" contains pseudorandom
** imperfections specified at the nodes in the z-direction. This file is
** called from the main input file named ‘‘Tension-membrane.inp".
**

**  X, Y, and Z imperfections to be added to the nodal coordinates

    1,   0.00000E+00,   0.00000E+00,   0.18225E-02
    2,   0.00000E+00,   0.00000E+00,  -0.18096E-02
    3,   0.00000E+00,   0.00000E+00,   0.28307E-03
    4,   0.00000E+00,   0.00000E+00,   0.49976E-03
    5,   0.00000E+00,   0.00000E+00,   0.25069E-02
    6,   0.00000E+00,   0.00000E+00,  -0.83239E-03
**
**     To shorten the input listing, numerous data
**     lines are not shown. There are 1323 nodes in this model.
**
 1316,   0.00000E+00,   0.00000E+00,   0.31476E-03
 1317,   0.00000E+00,   0.00000E+00,  -0.22987E-02
 1318,   0.00000E+00,   0.00000E+00,  -0.11013E-03
 1319,   0.00000E+00,   0.00000E+00,   0.33677E-03
 1320,   0.00000E+00,   0.00000E+00,  -0.22062E-02
 1321,   0.00000E+00,   0.00000E+00,  -0.21439E-03
 1322,   0.00000E+00,   0.00000E+00,  -0.13981E-02
 1323,   0.00000E+00,   0.00000E+00,  -0.10384E-02
```

Acknowledgments

The authors thank J. Leifer, University of Kentucky, and J. Blandino, James Madison University, for providing the experimental results.

References

[1]Chmielewski, A. B., “Overview of Gossamer Structures,” *Gossamer Spacecraft: Membrane and Inflatable Structures Technology for Space Applications*, edited by C. H. M. Jenkins, Vol. 191, Progress in Astronautics and Aeronautics, AIAA, Reston, VA, 2001, pp. 1–33.

[2]Wagner, H., “Flat Sheet Metal Girders with Very Thin Metal Web,” *Zeitschrift für Flugtechnik und Motorluftschiffahrt*, Vol. 20, 1929, pp. 200–314.

[3]Reissner, E., “On Tension Field Theory.” *Proceedings of the 5th International Congress on Applied Mechanics*, Wiley, 1938, pp. 88–92.

[4]Kondo, K., Iai, T., Moriguti, S., and Murasaki, T., “Tension-Field Theory,” *Memoirs of the Unifying Study of Basic Problems in Engineering Science by Means of Geometry*, Vol. 1, Gakujutsu, Bunken Fukyo-Kai, Tokyo, 1955, pp. 61–85.

[5]Mansfield, E. H., “Load Transfer via a Wrinkled Membrane,” *Proceedings of the Royal Society of London*, Vol. 316, 1970, pp. 269–289.

[6]Stein, M., and Hedgepeth, J. M., “Analysis of Partly Wrinkled Membranes,” NASA TN D-813, July 1961.

[7]Wu, C. H., and Canfield, T. R., “Wrinkling in Finite Plane Stress Theory,” *Quarterly of Applied Mathematics*, Vol. 39, 1981, pp. 179–199.

[8]Pipkin, A. C., “The Relaxed Energy Density for Isotropic Elastic Membranes,” *Journal of Applied Mathematics*, Vol. 36, 1986, pp. 85–99.

[9]Steigmann, D. J., and Pipkin, A. C., “Wrinkling of Pressurized Membranes,” *Journal of Applied Mechanics*, Vol. 56, 1989, pp. 624–628.

[10]Miller, R. K., and Hedgepeth, J. M., “An Algorithm for Finite Element Analysis of Partly Wrinkled Membranes,” *AIAA, Journal*, Vol. 20, 1982, pp. 1761–1763.

[11]Adler, A. L., Mikulas, M. M., and Hedgepeth. J. M., “Static and Dynamic Analysis of Partially Wrinkled Membrane Structures,” AIAA Paper 2000-1810, April 2000.

[12]Schur, W. W., “Tension-field Modeling by Penalty Parameter Modified Constitutive Law,” Proceedings of the 24th Midwestern Mechanics Conf., Ames, IA, Oct. 1995.

[13]Liu, X., Jenkins, C. H., and Schur, W. W., “Large Deflection Analysis of Pneumatic Envelopes Using a Penalty Parameter Modified Material Model,” *Finite Elements in Analysis and Design*, Vol. 37, No. 3, 2001, pp. 233–251.

[14]Liu, X., Jenkins, C. H., and Schur, W. W., “Fine Scale Analysis of Wrinkled Membranes,” *International Journal of Computational Engineering Science*, Vol. 1, No. 2, 2000, pp. 281–298.

[15]Blandino, J. R., Johnston, J. D., Miles, J. J., and Dharamsi, U. K., “The Effect of Asymmetric Mechanical and Thermal Loading on Membrane Wrinkling,” AIAA Paper 2002-1371, April 2002.

[16]Johnston, J. D., “Finite Element Analysis of Wrinkled Membrane Structures for Sunshield Applications,” AIAA Paper 2002-1456, April 2002.

[17]Lo, A., “Nonlinear Dynamic Analysis of Cable and Membrane Structures,” Ph.D. Dissertation, Oregon State Univ., Corvalis, OR, Dec. 1981.

[18]Jenkins, C. H., and Leonard, J. W., “Dynamic Wrinkling Of Viscoelastic Membranes,” *Journal of Applied Mechanics*, Vol. 60, Sept. 1993, pp. 575–582.

[19]“ABAQUS/Standard User’s Manual,” Ver. 6.3.1, Hibbitt, Karlsson, and Sorensen, Inc., Pawtucket, RI, 2002.

[20]Lee, K., and Lee, S. W., “Analysis of Gossamer Space Structures Using Assumed Strain Formulation Solid Shell Elements,” AIAA Paper 2002-1559, April 2002.

[21]Wong, Y. W., and Pellegrino, S., “Computation of Wrinkle Amplitudes in Thin Membranes,” AIAA Paper 2002-1369, April 2002.

[22]Leifer, J., Black, J. T., Belvin, W. K., and Behun, V., “Evaluation of Shear Compliant Boarders for Wrinkle Reduction in Thin Film Membrane Structures,” AIAA Paper 2003-1984, April 2003.

[23]Blandino, J. R., Johnston, J. D., and Dharamsi, U. K., “Corner Wrinkling of a Square Membrane Due to Symmetric Mechanical Loads,” *Journal of Spacecraft and Rockets*, Vol. 35, No. 5, 2002, pp. 717–724.

[24]Tessler, A., “A Priori Identification of Shear Locking and Stiffening in Triangular Mindlin Elements,” *Computer Methods in Applied Mechanics and Engineering*, Vol. 53, No. 2, 1985, pp. 183–200.

T. Collins
Associate Editor